JACS
JOURNAL OF THE AMERICAN CHEMICAL SOCIETY
Article
pubs.acs.org/JACS

Single Molecule Characterization of the Interactions between Amyloid-β Peptides and the Membranes of Hippocampal Cells

Priyanka Narayan,[†,⊥] Kristina A. Ganzinger,[†,⊥] James McColl,[†,#] Laura Weimann,[†] Sarah Meehan,[†] Seema Qamar,[‡] John A. Carver,[§] Mark R. Wilson,[∥] Peter St. George-Hyslop,[‡] Christopher M. Dobson,*[,†] and David Klenerman*[,†]

[†]Department of Chemistry, University of Cambridge, Lensfield Road, Cambridge, United Kingdom CB2 1EW

[‡]Cambridge Institute for Medical Research, Wellcome Trust/MRC Building, Addenbrooke's Hospital, Hills Road, Cambridge, United Kingdom CB2 0XY

[§]School of Chemistry and Physics, University of Adelaide, Adelaide, South Australia 5005, Australia

[∥]School of Biological Sciences, University of Wollongong, Wollongong, New South Wales 2522, Australia

Supporting Information

ABSTRACT: Oligomers of the 40 and 42 residue amyloid-β peptides (Aβ40 and Aβ42) have been implicated in the neuronal damage and impaired cognitive function associated with Alzheimer's disease. However, little is known about the specific mechanisms by which these misfolded species induce such detrimental effects on cells. In this work, we use single-molecule imaging techniques to examine the initial interactions between Aβ monomers and oligomers and the membranes of live cells. This highly sensitive method enables the visualization of individual Aβ species on the cell surface and characterization of their oligomerization state, all at biologically relevant, nanomolar concentrations. The results indicate that oligomers preferentially interact with cell membranes, relative to monomers and that the oligomers become immobilized on the cell surface. Additionally, we observe that the interaction of Aβ species with the cell membrane is inhibited by the presence of ATP-independent molecular chaperones. This study demonstrates the power of this methodology for characterizing the interactions between protein aggregates and the membranes of live neuronal cells at physiologically relevant concentrations and opens the door to quantitative studies of the cellular responses to potentially pathogenic oligomers.

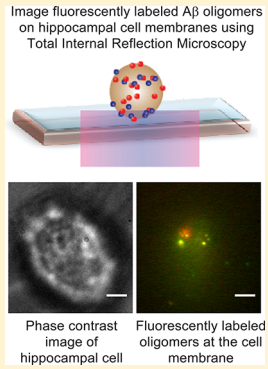

INTRODUCTION

Proteinaceous deposits, primarily comprised of plaques of amyloid-β peptides (Aβ), are a pathological hallmark of Alzheimer's disease (AD) and are present in the brains of patients at the later stages of AD. Recent research has suggested, however, that soluble oligomers of Aβ are the primary origin of neuronal damage and decline in cognitive function associated with the disease.[1−10] Of the numerous suggested mechanisms of Aβ-mediated neurotoxicity, many include interactions with a variety of cellular components and, in particular, with cell membranes.[11−16] Therefore, in order to understand the detrimental effects of Aβ aggregates, it is crucial to characterize the earliest events in the pathogenic process, namely the interactions between Aβ and cellular membranes.

One of the primary challenges in resolving the detailed mechanism of Aβ-mediated neurotoxicity is the heterogeneous nature of the Aβ species formed during the aggregation reaction. Conventional biochemical techniques provide information about the overall behavior of the ensemble of species present in a given sample, from which it is challenging to define the roles of specific components within the ensemble. In this study, therefore, we have used single-molecule imaging to visualize individual Aβ species and to differentiate between monomers and the various types of oligomers observed in these experiments. Specifically, the application of total internal reflection fluorescence microscopy (TIRFM) enables us to study the cell-surface interactions resulting from the exogenous application of well-characterized Aβ assemblies and to investigate their diffusional behavior on the cell surfaces. Employing the same methodology, we have also been able to examine the effects of molecular chaperones on the interaction of Aβ species with cell membranes.

TIRFM enables the observation of species at the cell membrane specifically as fluorescent signals are collected only at the interface of the coverslip and the sample placed upon it; if a cell is present in this illuminated region, any fluorescent species attached to the cell membrane will be detected. Moreover, these experiments can be performed at concentrations as low as 1 nM, enabling investigations to be carried out at near-endogenous Aβ concentrations (1−10 nM).[17] In this work, we have performed a detailed biophysical characterization of the interactions between oligomers of the 40 and 42 residue isoforms of Aβ (Aβ40 and Aβ42 respectively) and the membranes of live neuronal cells in order to enable comparisons to be made between the effects of the two peptides. As the hippocampus is the part of the brain

Received: October 19, 2012
Published: January 22, 2013

   dx.doi.org/10.1021/ja3103567 | J. Am. Chem. Soc. 2013, 135, 1491−1498

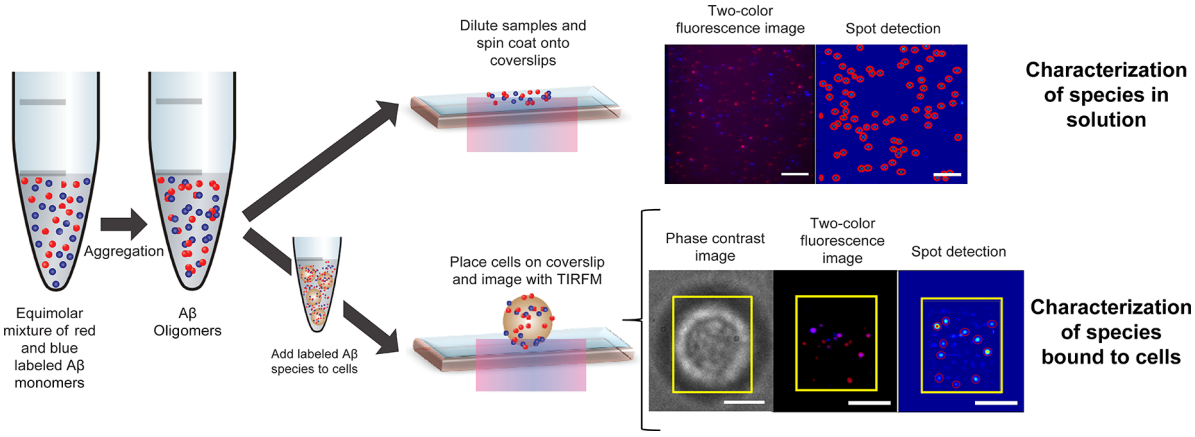

Figure 1. Schematic diagram of the single-molecule methods used to detect species in solution (top) and those interacting with cell membranes (bottom). Black panels are two-color fluorescence images and blue panels show spot detection in red circles. All scale bars are 5 μm.

most notably affected in AD, an immortalized murine hippocampal neuronal cell line (HpL) was chosen for these studies.[18]

To generate oligomers of the Aβ peptides which could be observed by TIRFM, equimolar quantities of monomeric Aβ (labeled with either a HiLyteFluor488 or a HiLyteFluor647 fluorophore) were combined and allowed to aggregate for a period of time which previous work has shown to generate oligomers.[19] Earlier studies have also confirmed that the attachment of these fluorescent tags at the N-terminus of the peptide does not significantly affect the aggregation properties of the Aβ peptides.[19−21] Within the aggregation mixture, the oligomers can be distinguished from monomers by selecting for species containing two differently colored fluorophores, whereas monomers are tagged with only a single fluorophore, either HiLyteFluor488 or HiLyteFluor647. Thus, when the oligomer mixtures were observed using two-color TIRFM, it is straightforward not only to count the number of Aβ species present but also to characterize each of these species as a monomer or an oligomer by analyzing the spatial coincidence of the fluorescent signals of different colors (see Supporting Information and Figures 1 and S1). Additionally, we could gain an added dimension of detail by using the fluorescence intensity of the dual-color oligomers to estimate their size[20,21] (see Supporting Information and Figure S2). We have performed this characterization for Aβ species present in the aggregation mixtures as well as for those which interact with cell membranes after incubating the Aβ mixtures with neuronal cells (Figure 1). Since TIRFM is highly sensitive to nonspecific binding of molecules to the surface under observation, it was important to develop a robust protocol which enabled us to observe cell-specific Aβ interactions while minimizing the nonspecific adhesion of Aβ species to the coverslip (Figure 2).

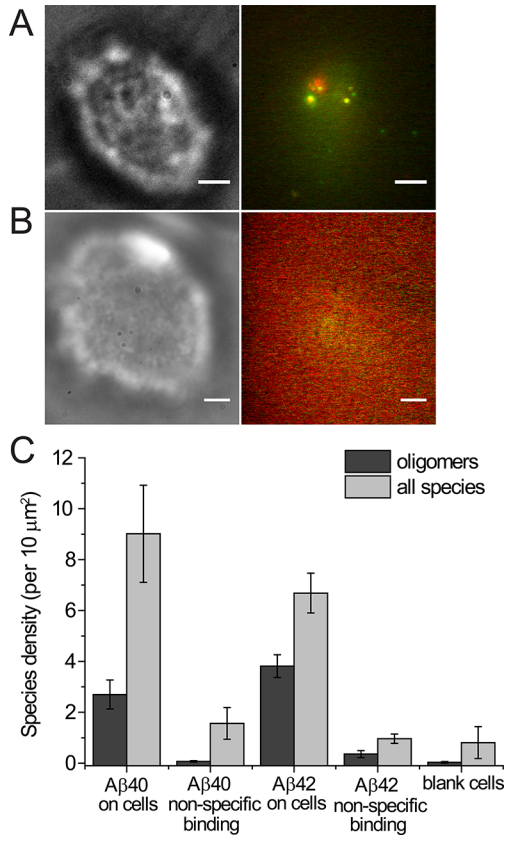

Figure 2. Representative images of HpL cells incubated with (A) and without (B) 500 nM of fluorescently labeled Aβ42 that has undergone aggregation for 3−4 h. In each pair of images, the left is the phase contrast image, and the right is the fluorescent (TIRFM) image. Yellow species in the fluorescent image are oligomers (dually labeled), whereas green and red species are monomers (singly labeled). Scale bars are 3 μm. (C) Aβ40 and Aβ42 monomeric and oligomeric species were detectable over the limits of nonspecific interaction with the slide surface and over the background fluorescence of unlabeled cells 500 nM total peptide concentration, number of cells varied from 35 to 50 for each category, error bars are standard error of the mean, (SEM).

EXPERIMENTAL SECTION

Cell Culture. Murine hippocampal HPL (P4, Prnp−/−) cells were cultured in Opti-MEM media (GIBCO) supplemented with 10% fetal bovine serum (Sigma St. Louis, MO) and 1% penicillin/streptomycin (GIBCO, Carlsbad, CA) in a 5% CO_2 environment at 37 °C.[18] These cells do not express the prion protein receptor (PrP^C), which, recently, has been suggested to mediate the cellular toxicity of Aβ peptides. We used this cell line to examine the basal levels of Aβ binding to a model surface in the absence of the influence of this putative receptor.

Aβ Peptide Preparation. Monomeric solutions of HiLyteFluor488 and HiLyteFluor647-labeled Aβ40 or Aβ42 (Anaspec, San Jose, CA) were prepared by dissolving the lyophilized peptide in 0.01 M NaOH followed by sonication over ice for 30 min (Bandelin Sonorex, Schalltec Morfelden-Walldorf, Germany) and subsequent flash freezing into aliquots.[22] Prior to each of the incubations, aliquots of each peptide were brought to pH 7.4 by diluting into SSPE buffer (150 mM NaCl, 10 mM NaH_2PO_4, 10 mM Na_2EDTA, pH 7.4) to the desired concentration and placed under the chosen conditions for aggregation (37 °C, agitation, 1

dx.doi.org/10.1021/ja3103567 | J. Am. Chem. Soc. 2013, 135, 1491−1498

and 2 μM of Aβ42 and Aβ40, respectively, for time dependence measurements and 10 and 20 μM of Aβ42 and Aβ40, respectively, for concentration dependence experiments). The concentration of each labeled peptide was measured before mixing using confocal two-color-coincidence detection (cTCCD).[19] The peptides were aggregated for 3−4 h at lower concentrations (1 or 2 μM) for time dependence measurements and aggregated for 1 h at higher concentrations (10 or 20 μM) for concentration dependence experiments.

TIRFM Instrumentation. Imaging was performed using TIRFM by aligning the outputs from a HeNe laser operating at 633 nm (25LHP991230, Melles Griot, Albuquerque, NM) and a diode laser operating at 488 nm (PC13589, Spectra Physics, Santa Clara, CA) and directing them down the edge of a TIRF objective (60× Plan Apo TIRF, NA 1.45, Nikon Instruments, New York, NY) mounted on a Nikon Eclipse TE2000-U microscope. Fluorescence collected by the same objective was separated from the returning TIR beam by a dichroic (FF500/646-Di1, Semrock, Rochester, NY), split into blue and red components (585 DXLR, Omega Optical, Brattleboro, VT) and filtered using Dual-View (Optical Insights, Lilburn, CA) mounted filters. The images were simultaneously recorded on an EMCCD camera (Cascade II: 512, Photometrics, Tuscon, AZ) operating at −70 °C, whereby the emission signal from the 488 and 647 nm fluorophores was split so that each color was recorded on one-half of the EMCCD chip (Dual-View, Photometrics, Roper Scientifics, Tuscon, AZ) with a pixel size of 106 nm. Data were acquired at 28.6 frames s^{-1} using Micromanager.[23] To achieve good image registration, a grid consisting of regularly spaced ion-beam etched holes in gold-on-glass was utilized. The Dual-View optics were adjusted so as to maximize the overlap of the images of the grid in the two channels under white-light illumination, resulting in a measured mean image registration of approximately 100 nm.

Characterization of Aβ in Solution. Solutions containing labeled Aβ monomers and/or oligomers (prepared as described above) were diluted to a total peptide concentration of 1 nM in PBS (see Figure 1) and spin coated onto glass coverslips (2000 rpm, 1 min, model WS-400B-6NPP/Lite, Laurell Tech., North Wales, PA) for imaging. The intensity of the excitation laser(s) was adjusted so that single fluorophores (monomers) could be efficiently discriminated against the background. The microscope coverslips had been incubated for 1 h in piranha solution (3:1 sulfuric acid:hydrogen peroxide), thoroughly rinsed with ultrapure water (Milli-Q, 18.2 MΩ resistance), and subsequently cleaned with oxygen plasma for 2 min (Femto, Electronic Diener, Royal Oak, MI).

Characterization of Aβ on Cells. At least 24 h prior to experiments, cells were seeded in six-well plates (Delta plates, NUNC). For the experiments, cells were incubated with sterile PBS (12 min, 37 °C) after which they could be easily removed from the surface by aspirating with a pipet. Cells were resuspended in DMEM/10% FCS or Opti-MEM/10% FCS and incubated in an Eppendorf tube for 15 min at 37 °C with the fluorophore-labelled Aβ solutions containing monomers and/or oligomers, at the concentrations described in the text. For experiments with chaperones, the Aβ40 samples were preincubated with equimolar amounts of αB-crystallin or clusterin for at least 15 min at room temperature. Then these mixtures were added to the cell suspensions. Following incubation, the cells were washed twice with the culture media and once with PBS by centrifugation and resuspension of the pellet (600 × *g*, 2 min). Prior to imaging, coverslips were cleaned as described above and subsequently coated with a 1 mg/mL solution of PLL(20)-g[3.7]-PEG(2.3)/PEG(3.4)-RGD(12%) (PLL-PEG-RGD) (SuSoS, AG, Switzerland) for 10 min at room temperature.[24−26] Any unbound PLL-PEG-RGD was then thoroughly washed off using PBS. This coating allowed the cells to bind to the functionalized surface via their integrin receptors, and the polyethyleneglycol reduced the nonspecific Aβ adherence to the coverslip by a factor of 50. With this protocol we were able to ensure that the only Aβ species observed were those bound to the cells under observation. Slides were transferred to the microscope stage, and the cells were added, allowed to settle for 5 min, and then imaged within the subsequent 20 min at room temperature. Due to the washing steps involved in the sample preparation, we could not ensure that these measurements were taken at equilibrium. Therefore, we have chosen to make comparisons between values of the measured parameters rather than analyzing the absolute values.

Preparation of Chaperones. Human recombinant αB-crystallin was prepared as described previously.[27] Clusterin was extracted from human serum from Wollongong Hospital (Wollongong, NSW, Australia), as described previously.[28]

Particle Detection. Images were analyzed using custom-written software (MATLAB). With this software, the user interactively selects boundaries for each cell based on white light images acquired during the data collection phase. The corresponding fluorescence images were then band-pass filtered, and a threshold for the subsequent spot detection was determined from the background. First, a distribution of values of the median background fluorescence was determined, and spots were identified as species having a brightness value greater than the sum of the median background fluorescence and twice the interquartile range of the background. This threshold was empirically determined with a number of test samples including monomeric Aβ on glass coverslips and cells. Detection of spots corresponding to Aβ oligomers was performed using first a centroid and subsequently a Gaussian fit to bright objects with spot intensities corrected for the local background then extracted. Large oligomers were distinguished from closely associated monomers by defining a maximum allowed ellipticity for a detected particle. A few cells were observed to have fibrillar species bound to them (Figure S3). These were discarded from the analysis as they represented a small fraction of the total population of cells and because oligomers have been identified as the key toxic species.[10]

Particle Tracking and Diffusion Analysis. The positions of each particle in each frame were recorded, and the spots were tracked using custom-written MATLAB code which linked the spot positions from frame to frame by an implementation of the IDL particle tracking function defined by Crocker and Grier.[29] The trajectories were then analyzed using two approaches, a mean-square displacement (MSD) analysis and a jump−distance (JD) analysis.

For the MSD analysis, the MSDs over the first five time intervals were calculated, and individual diffusion coefficients obtained, using the linear relationship between MSD and a given time interval between frames *dt*.[30] Briefly, for each recorded trajectory (points $\{x(i), y(i)\}$), MSD values were calculated using the method described by Qian et al. and Saxton and Jacobsen.[31,32] They define the MSD for a given time lag *ndt* as the average over all points with that time lag:

$$\mathrm{MSD}(ndt) = \frac{1}{l-n}\sum_{i=1}^{l-n}[x(i+n)-x(i)]^2 + [y(i+n)-y(i)]^2 \quad (1)$$

with l denoting the trajectory length and dt the time step between frames. It holds that

$$\mathrm{MSD}(ndt) = 4Dndt + \mathrm{offset} \quad (2)$$

with D denoting the short-term diffusion coefficient; the gradient of a linear fit for $n \leq 5$ is therefore proportional to D. A weighted fit was used as errors are assumed to be approximately normally distributed.

For the JD analysis, the distances between particle positions in subsequent frames, the so-called jump distances, were calculated, and compiled into histograms. These histograms reflect the probability distribution of the distance that a particle moves in the set time between frames, and this distribution can be fitted with a linear combination of the two-dimensional diffusion equation to extract diffusion coefficients of multiple diffusing populations[30,33,34].

$$p(r) = \sum_{j=1}^{m}\frac{Mf_j}{2D_j dt}\mathrm{e}^{-r^2/4D_j dt}rdr \quad (3)$$

The MSD analysis of the trajectories was additionally used to obtain an estimate for the diffusion coefficients of individual oligomers in order to correlate diffusion and oligomer brightness.

Size Determination. Since almost all of the oligomers were found to be static, their positions and intensities were averaged over multiple frames before bleaching occurred. Coincident spots were detected by calculating the distance between the spots in the blue and red

dx.doi.org/10.1021/ja3103567 | J. Am. Chem. Soc. 2013, 135, 1491−1498

channels.[35] Here we required associated particles to stay within 300 nm of each other to account for imperfections in image registration (Figure S1). First, the mean brightness of a red monomer I_{mon} was estimated by analyzing bleaching traces manually using ImageJ (NIH, freeware, Figure S2). Then the fluorescence intensity collected from the 633 nm excitation channel I_{633} for each coincident spot detected was doubled and then scaled by the monomer brightness determined by photobleaching, and the size of the spot was expressed in terms of numbers of monomers. This method assumes that no quenching takes place in higher oligomers, which has been found to be a good approximation up to ca 20-mers.[21]

$$\text{size} = \frac{I_{633} \times 2}{I_{mon}} \tag{4}$$

The size distribution was then corrected for the undetected (single color) fraction of oligomers (e.g., single-color dimers, trimers, etc.) from the binomial probabilities of detection. The correction factor (F) for a given oligomer size n, as given below, is less than 1% for oligomers over 7-mers in size:

$$F_n = \frac{\sum_0^n C_x^n}{1 - (C_0^n + C_n^n)} \tag{5}$$

Then the total number of oligomeric spots $[\sum_0^{50}(F_n \times N_n)]$ was determined following this correction. This was taken as a fraction of the total number of species detected N_{total} for all plots where quantities are expressed as fractions:

$$N_{total} = (N_{633} + N_{488}) - \sum_0^{50} (F_n \times N_n) \tag{6}$$

Further statistical analysis was performed using Origin (OriginLab).

RESULTS

Oligomers of Aβ40 and Aβ42 Preferentially Interact with the Cell Membrane Relative to Aβ Monomers. With the confidence that only specific interactions between the Aβ peptides and the cell membranes are observed by this technique (Figure 2), we examined whether the distribution of species of Aβ present in solution was different from the distribution of Aβ species interacting with cell membranes. To this end, we incubated the cells with solutions of Aβ (both Aβ40 and Aβ42) that had been allowed to aggregate for various periods of time and concurrently characterized the solution in the absence of cells by spin-coating the solution onto a glass coverslip and imaging both samples using dual-excitation TIRFM. Previous studies have confirmed that characterization of oligomer formation by this method accurately describes the species found in solution.[19]

We then quantified the number and sizes of Aβ species in solution before and after incubation with cells. We accomplished this objective by using TIRFM first to characterize a solution of Aβ species containing both oligomers and monomers. Then this same solution was added to a suspension of cells, incubated with the cells for at least 15 min, and then the cells were separated from the soluble medium via centrifugation. The cells were then visualized using TIRFM, and the species on the cell surface were characterized as monomers or oligomers. Both monomers and oligomers were observed to interact with the surfaces of the cells. We then compared the oligomeric fraction of the Aβ40 or Aβ42 (number of oligomers relative to the total species) present in solution with the fraction of the oligomeric Aβ40 or Aβ42 species interacting with the cell membrane. This analysis revealed that the fraction of Aβ40 or Aβ42 oligomers interacting with the cell membrane was 5−7-fold greater than their fraction observed in solution (Figure 3, A,B, paired two-tailed t test, $p < 0.01$).

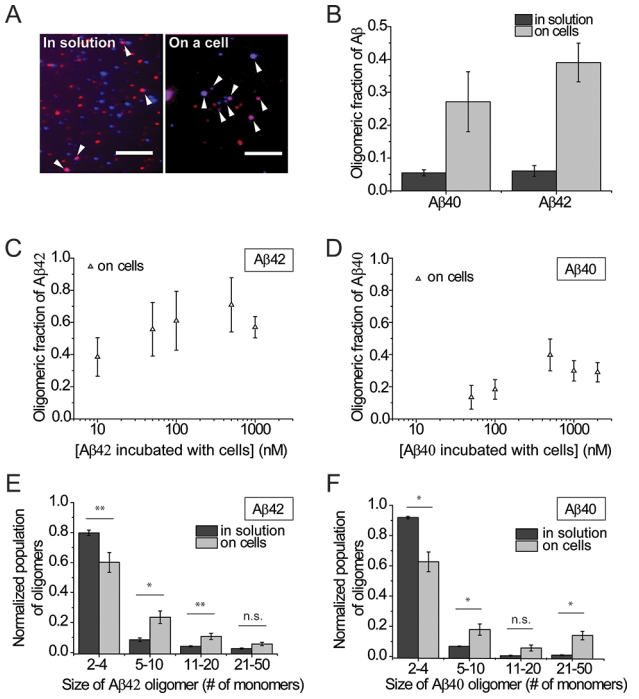

Figure 3. (A) Representative TIRFM images with arrows depicting the increased fraction of Aβ oligomers on the surfaces of hippocampal cells. The oligomeric fraction of Aβ42 and Aβ40 (B) on cell membranes and in solution prior to incubation with cells (aggregation concentrations used were 1 μM Aβ42 and 2 μM Aβ40); Aβ species were analyzed at different times during the aggregation reaction. For characterization of species prior to incubation with cells, the data were derived from three separate incubations. The oligomeric fraction of Aβ interacting with cell membranes as a function of different incubation concentrations of Aβ42 (C) and Aβ40 (D) (ANOVA single factor $p = 0.17$ for Aβ40 and $p = 0.65$ for Aβ42); distribution of sizes of oligomers after 4 h of aggregation of Aβ42 (E) or Aβ40 (F) present in solution (prior to incubation with cells) and on cell membranes (aggregation concentrations used were 1 μM Aβ42 and 2 μM Aβ40, $n = 30-50$ cells). All error bars are SEM; * is $p < 0.05$; ** is $p < 0.01$; n.s. $p > 0.05$.

Since the numbers of oligomeric species and their size distributions are dependent on the progress of the aggregation reaction, we next examined whether or not the enrichment of oligomers at the cell surface changed with the time that Aβ40 and Aβ42 were left to aggregate in the absence of cells. We found that the increase in oligomeric fraction of Aβ at the cell surfaces (compared to that in solution) was similar for Aβ40 and Aβ42 having undergone aggregation for times ranging from 2 to 12 h. The oligomeric fractions of Aβ40 and Aβ42 present on cell membranes were not found to be significantly different from each other (p = 0.33, two sample independent t test). We were interested in whether the concentration of Aβ (40 or 42) in the incubation mixture with the cells affects the oligomeric fraction of Aβ interacting with the cell membrane. Varying the concentration of Aβ40 or Aβ42 (taken at a fixed time during the aggregation) in the solution in which the cells were incubated did not significantly change the oligomeric fraction of either isoform interacting with the cells (Figure 3C,D, ANOVA, single factor, p = 0.83, Figure S5). For both Aβ40 and Aβ42, the size distribution of the oligomeric species that were associated with cell surfaces was skewed toward larger species than those present in solution (Figure 3E,F), a finding in accord with other work on Aβ40.[20]

The increased oligomeric fraction of Aβ (of both isoforms) observed on the cell membrane, relative to the oligomeric

dx.doi.org/10.1021/ja3103567 | J. Am. Chem. Soc. 2013, 135, 1491−1498

fraction of Aβ in solution, reflects a preferential adherence of oligomers (over monomers) to the cell membrane. This increased fraction is not due to further aggregation of Aβ in solution during the incubation with the cells; we can exclude this mechanism because the difference in the oligomeric fraction of Aβ in solution and on cells is far greater than the difference in the oligomeric fraction of Aβ observed in solution over the entire aggregation reaction. Aβ oligomers possess a greater amount of solvent-exposed hydrophobic surface area than monomers, a property which may favor their interaction with cell membranes and has also been correlated with their cellular toxicity.[36]

Mobility of Aβ40 and Aβ42 Oligomers is Inversely Correlated with Oligomer Size. Having established that the relative levels of oligomeric species are enriched at cell membranes compared to the solution phase, we then investigated the nature of the interaction with the membranes. As our technique enables visualization of single-Aβ species and characterization of their oligomer state, we examined whether or not there were any differences in the mobility of oligomers and monomers in the cell membrane. To accomplish this objective, we acquired videos of the Aβ species on cell surfaces. Since oligomers are likely to contain two differently colored fluorophores (HiLyteFluor488 and HiLyteFluor647), excitation with a 488 nm laser will result in fluorescence resonance energy transfer (FRET) between the two fluorophores and therefore a fluorescent signal from both detection channels. Therefore, we acquired the videos using single-color excitation (488 nm) for the TIRFM. Then, single-particle tracking algorithms were used to link the images of these species in subsequent frames within each video, thus obtaining trajectories of individual Aβ species in the cell membrane (representative frames shown in Figure 4A,B and video in Supporting Information).

First an analysis of the mean-square displacements (MSD) of each trajectory was used to estimate the diffusion coefficients of each molecule (Figure 4C). The average fluorescence intensity of each molecule was extracted simultaneously with the estimation of its diffusion coefficient (see Experimental section). Since the fluorescence intensity of an Aβ species is correlated with its size, the simultaneous estimation of intensity and diffusion coefficient allows us to investigate whether or not there is a relationship between the size of an Aβ assembly and its mobility in the cell membrane. Using the diffusion coefficients obtained from the MSD approach, we observed a clear negative correlation between the diffusion rate of a single Aβ species and its size (as assessed by its intensity). This observation holds for both Aβ40 and Aβ42 (Figure 4D). For Aβ40, we observe a subpopulation of small, fast-diffusing species. We can identify these species as monomeric since they do not undergo FRET and have low fluorescence intensities. If only the species that undergo FRET (i.e., oligomers) of both Aβ40 and Aβ42 are examined, the small, fast-diffusing population is not observed (Figure 4E). Interestingly the diffusion coefficients of the oligomers are small, and their trajectories indicate confined motion[32] (Figure 4A,B,E).

Mobility of Oligomers of Aβ40 and Aβ42 in the Cell Membrane is Highly Restricted. Extracting diffusion coefficients using an MSD analysis can be challenging for heterogeneous samples with multiple mobility populations and short trajectory lengths. Therefore the diffusion coefficients obtained using the MSD approach should be considered as approximate rather than exact values. In order to quantify the diffusion of the Aβ species interacting with the cell, we employed a second approach called JD analysis.[30,33,34,37] For this analysis a histogram of the displacement of a particle in a given time interval (jump-distance) is created. This histogram corresponds to the probability of a particle moving a certain distance in a given time; we can therefore fit this histogram with the two-

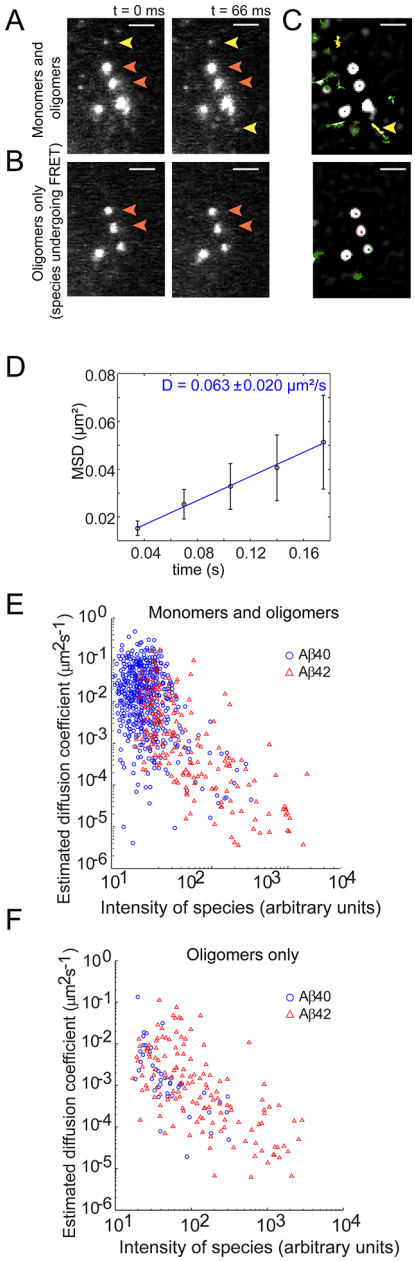

Figure 4. (A,B) Representative frames taken from a live cell imaging experiment to monitor Aβ40 diffusion in the cell membrane; the Aβ40 molecules were labeled with HiLyte488 and HiLyte647 fluorophores. (A) Monomers and oligomers (488 channel); (B) species undergoing FRET (633 nm channel, Aβ oligomers). The trajectories obtained by linking the images of the Aβ species in (A) and (B) are shown in (C). From the ensemble plots, it is already apparent that, in contrast to the small species present in (A), the motion of the large oligomers (defined as species that undergo FRET) is highly restricted. (D) A representative plot of the MSDs as a function of time for a mobile Aβ40 species (yellow arrows and trajectories in (C); the diffusion coefficient obtained from the fit is $D = 0.063 \pm 0.020$ $\mu m^2/s$. (E) The diffusion coefficient as estimated by the MSD analysis as a function of species intensity (which correlates with size) for both Aβ42 and Aβ40. Each point represents an Aβ monomer or oligomer. (F) The estimated diffusion coefficient as a function of species intensity for only the oligomers of Aβ42 and Aβ40. Concentrations used are 1 μM Aβ42 and 2 μM Aβ40.

dx.doi.org/10.1021/ja3103567 | J. Am. Chem. Soc. 2013, 135, 1491−1498

dimensional diffusion equation (see Experimental section). In this way, multiple diffusing populations can be resolved using a linear combination of the two-dimensional diffusion equation with varying diffusion coefficients, D, representing the various mobility populations, and amplitudes, A, representing the relative abundance of these populations.

When we applied the JD analysis to our data, we found that a minimum of three mobility populations was required to fit the experimentally derived JD distributions for both Aβ40 (D_2, D_3, D_4) and Aβ42 (D_1, D_2, D_3) (adjusted R^2 = 0.94 for two populations compared to R^2 = 0.98 for three populations). The majority of the Aβ40 and Aβ42 species interacting with the cell membrane were found to be either confined (D_1, D_2 between 0.00053−0.004 μm^2/s) or slow moving (D_3 between 0.038−0.050 μm^2/s) (Figure 5, and Table 1). For Aβ40, the fast-diffusing population (observed with the MSD approach) was identified as one of three mobility populations with an ensemble diffusion coefficient of D_4 = 0.225 ± 0.016 μm^2/s.

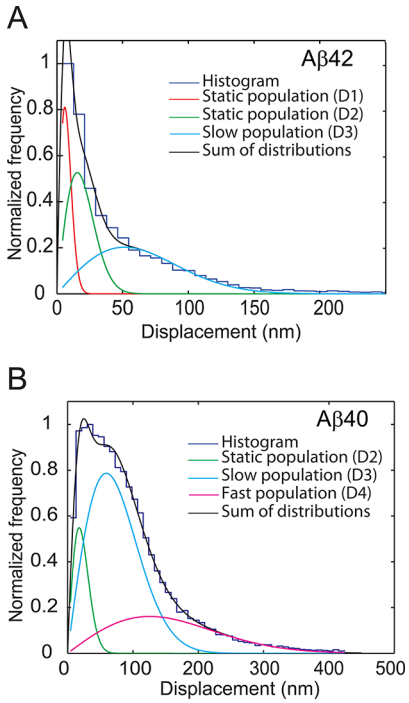

Figure 5. Distributions of particle displacements (JDs, blue histogram) per unit time (35 ms) of monomers and oligomers of Aβ42 (A) and Aβ40 (B) fit to the two-dimensional diffusion equation for three diffusing populations (eq 3, black line). The three components of the fit are shown in red, green, and cyan (A) and green, cyan, and purple (B), respectively. Concentrations used are 1 μM Aβ42 and 2 μM Aβ40.

We confirmed that this confinement was not an artifact of the TIRFM method since very little interaction exists between the oligomers and the coated coverslip, and species even larger than the oligomers observed have been found to move using TIRFM.[38] One possible explanation for the restricted diffusion of the majority of the oligomers of Aβ40 and Aβ42 is that the oligomers are attached to the membrane or a membrane component connected to the cytoskeletal framework of the cell. However, further investigation is required to explore this phenomenon in more detail.

Presence of ATP-Independent Chaperones Inhibits the Interaction Between Aβ40 and Cell Membranes. Having established a methodology for observing and characterizing the interaction of Aβ with cell membranes, we examined the way in which molecular chaperones can affect this process. The extracellular chaperone, clusterin, and the intracellular chaperone, αB-crystallin, act in an ATP-independent manner to inhibit protein aggregation in vitro and to suppress the cytotoxicity of amyloid-related oligomers.[39,40] Previous studies using single-molecule techniques have observed interactions between both of these chaperones and the Aβ40 peptide.[19,41] We therefore aimed to investigate whether or not the presence of these chaperones could modulate the interaction of Aβ40 with cell membranes. Solutions containing Aβ40 oligomers were first incubated with stoichiometric amounts of either clusterin or αB-crystallin and then added to the cells; we then quantified the number of oligomers and monomers interacting with the cells.

When comparing the species interacting with the cell surfaces in the presence and absence of the chaperones, it is apparent that the presence of either chaperone reduced the interaction of all Aβ40 species with cell membranes (Figure 6). This inhibition of binding may be attributable to the sequestration of Aβ40 species by these chaperones (as it has been previously observed in vitro) or as a result of interactions of the chaperone molecules themselves with the cell membrane. Further experiments will be needed to distinguish these and other possibilities, but in any case it is apparent that the presence of these chaperones reduces the number of oligomers interacting with the cellular membranes.

DISCUSSION

This work outlines a quantitative biophysical approach to studying the early stages of the interaction of Aβ species with the membranes of live cells. We have shown that oligomeric species interact preferentially with cell surfaces relative to monomeric peptides. The oligomeric fraction of Aβ42 interacting with the

Table 1. Diffusion Coefficients (D) and Relative Abundances (A) for All Experimental Conditions Studied in This Work

	D_1 (confined[a]) [μm^2/s]	A_1[%]	D_2 (confined[a]) [μm^2/s]	A_2 [%]	D_3 (slow) [μm^2/s]	A_2 [%]	D_4 (fast) [μm^2/s]	A_4 [%]
monomers and oligomers (Aβ42)	0.00053 ± 0.00001	21.2 ± 0.6	0.0040 ± 0.0002	32.5 ± 1.0	0.043 ± 0.001	46.3 ± 1.2	–	–
oligomers only (Aβ42)	0.00052 ± 0.00002	20.7 ± 0.9	0.0034 ± 0.0002	34.8 ± 1.2	0.038 ± 0.001	44.5 ± 1.2	–	–
monomers and oligomers (Aβ40)	–	–	0.0045 ± 0.0004	12.6 ± 0.7	0.050 ± 0.002	60.7 ± 2.0	0.226 ± 0.016	26.7 ± 2.3
oligomers only (Aβ40)	–	–	0.0045[b]	42.2 ± 1.5	0.0503[b]	57.8 ± 3.3	0.2256[b]	0.002 ± 0.025

[a]Note that these populations are confined within the localization precision of 34.4 ± 15.0 nm (see also Figure S1). [b]The values for D_1, D_2, and D_3 were fixed in order to enable a comparison of the fraction of species with varying mobility across all species of Aβ40 and Aβ40 oligomers only. Errors were calculated by bootstrapping using the size of the original data set and 1000 repetitions.

dx.doi.org/10.1021/ja3103567 | J. Am. Chem. Soc. 2013, 135, 1491−1498

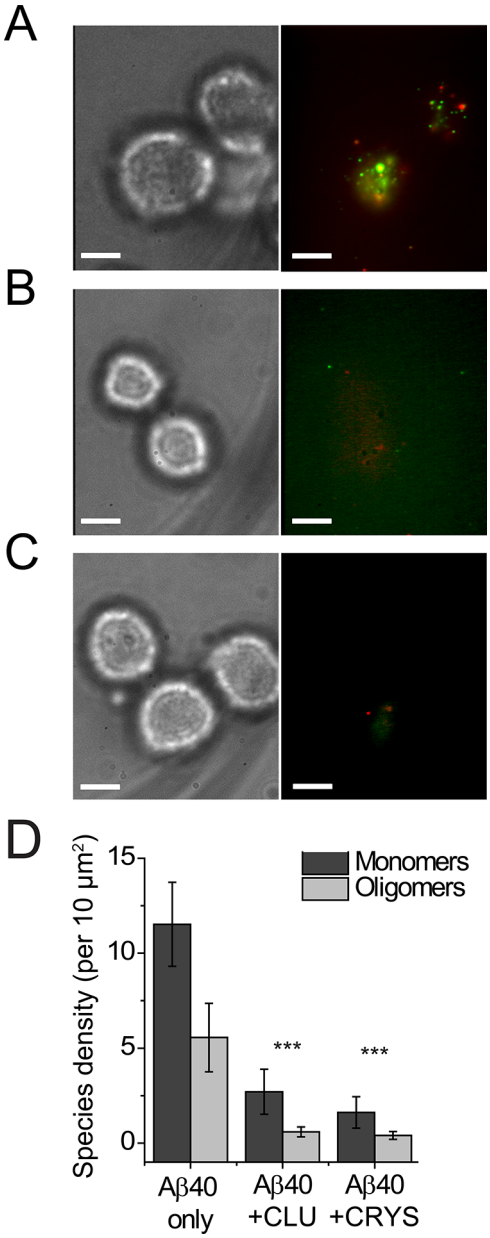

Figure 6. αB-Crystallin and clusterin inhibit the interaction of Aβ40 with the membranes of hippocampal cells. Representative TIRFM images of cells after incubation of the cells with fluorescently labeled Aβ40 monomers and oligomers in the absence of chaperones (A) or in the presence of either αB-crystallin (B) or clusterin (C). Phase contrast images are displayed (left) and fluorescence images (right). Single-color green or red species are HiLyteFluor488 and HiLyteFluor647-labeled Aβ40 monomers and dual-color species (which appears as yellow) are oligomers, the scale bar in each case is 5 μm. (D) The species density per 10 μm^2 cell area in the presence and absence of chaperones; 33−39 cells were analyzed for each sample. Significance testing was performed relative to "Aβ40 only", *** $p < 0.001$; * $p < 0.05$; n.s. $p > 0.05$. The concentrations used are 2 μM for Aβ40 and both chaperones. Error bars are SEM.

cell membrane is not significantly different from that of Aβ40, suggesting that oligomers of both peptides have a similar affinity for cell membranes. On the cell surface most oligomers of both isoforms display restricted motion, characterized by diffusion coefficients between 10^{-4} and 10^{-3} μm^2/s, values that are far lower than the diffusion coefficients of mobile transmembrane proteins (10^{-2} and 10^{-1} μm^2/s). This result suggests that the majority of the Aβ species are not bound to a mobile cell-surface protein and could be interacting with a more immobile partner, for example, a cytoskeleton-associated membrane component.[42,43] However, future investigations are needed to evaluate the causes of restricted diffusion in detail. Larger oligomers exhibit slower motion than smaller oligomers which could be a consequence of differential levels of membrane integration due to different degrees of exposed hydrophobic surface area.[36,44,45] Indeed, varying levels of exposed hydrophobic surface area have been correlated with different toxicity.[36] Moreover, the preincubation of oligomeric solutions of Aβ40 with either clusterin or αB-crystallin prior to their addition to cells prevents the interaction of the Aβ40 species with the cell surface.

This study illustrates a methodology with the potential to examine in detail how various biologically relevant molecules influence the interactions between the various Aβ species and cell membranes. While numerous cellular studies of Aβ examine effects at concentrations that are 100- and 1000-fold higher than those present physiologically, our use of single-molecule imaging enables us to work at near physiological, nanomolar concentrations, which are particularly relevant to the initial stages of Aβ-induced AD pathology.

■ ASSOCIATED CONTENT

Supporting Information

Characterization of localisation precision and monomer intensity, Supporting Figures 1−5.

The video is representative of those taken during the data acquisition process. HiLyte488 or 647 labeled Aβ interacts with the plasma membrane of live hippocampal cells (data shown after application of a band-pass filter). This material is available free of charge via the Internet at http://pubs.acs.org.

■ AUTHOR INFORMATION

Corresponding Author

cmd44@cam.ac.uk; dk10012@cam.ac.uk

Present Address

[#]School of Biological Sciences, University of East Anglia, Norwich Research Park, Norwich NR4 7TJ, United Kingdom

Author Contributions

[⊥]These authors contributed equally.

Notes

The authors declare no competing financial interest.

■ ACKNOWLEDGMENTS

P.N. is supported by a Marshall Scholarship from the Marshall Aid Commemoration Commission and a Graduate Research Fellowship from the National Science Foundation. K.A.G. is supported by fellowships from the EPSRC and Studienstiftung des deutschen Volkes. J.M. is supported by the Wellcome Trust. L.W. is supported by an EPSRC fellowship. S.M. is supported by a Royal Society Dorothy Hodgkin Fellowship. M.R.W. acknowledges the support of the Australian Research Council (DP0773555 and DP0984341). The research of S.Q., D.K., P.St.G.-H. and C.M.D. is supported by the Wellcome Trust and that of D.K. by the Augustus Newman Foundation. We thank Dr. Rohan T. Ranasinghe for stimulating discussions of this work and for critical reading of this manuscript.

REFERENCES

(1) Shankar, G. M.; Li, S. M.; Mehta, T. H.; Garcia-Munoz, A.; Shepardson, N. E.; Smith, I.; Brett, F. M.; Farrell, M. A.; Rowan, M. J.; Lemere, C. A.; Regan, C. M.; Walsh, D. M.; Sabatini, B. L.; Selkoe, D. J. *Nat. Med.* **2008**, *14*, 837.

(2) Selkoe, D. J. *Behav. Brain Res.* **2008**, *192*, 106.

(3) Näslund, J.; Haroutunian, V.; Mohs, R.; Davis, K. L.; Davies, P.; Greengard, P.; Buxbaum, J. D. *JAMA, J. Am. Med. Assoc.* **2000**, *283*, 1571.

(4) McLean, C.; Cherny, R.; Fraser, F.; Fuller, S.; Smith, M.; K, V.; Bush, A.; Masters, C. *Ann. Neurol.* **1999**, *46*, 860.

(5) Lue, L.-F.; Kuo, Y.-M.; Roher, A. E.; Brachova, L.; Shen, Y.; Sue, L.; Beach, T.; Kurth, J. H.; Rydel, R. E.; Rogers, J. *Am. J. Pathol.* **1999**, *155*, 853.

(6) Li, S.; Hong, S.; Shepardson, N. E.; Walsh, D. M.; Shankar, G. M.; Selkoe, D. *Neuron* **2009**, *62*, 788.

(7) Lacor, P. N.; Buniel, M. C.; Chang, L.; Fernandez, S. J.; Gong, Y.; Viola, K. L.; Lambert, M. P.; Velasco, P. T.; Bigio, E. H.; Finch, C. E.; Krafft, G. A.; Klein, W. L. *J. Neurosci.* **2004**, *24*, 10191.

(8) Haass, C.; Selkoe, D. J. *Nat. Rev. Mol. Cell Biol.* **2007**, *8*, 101.

(9) Chiti, F.; Dobson, C. M. *Annu. Rev. Biochem.* **2006**, *75*, 333.

(10) Bucciantini, M.; Giannoni, E.; Chiti, F.; Baroni, F.; Formigli, L.; Zurdo, J. S.; Taddei, N.; Ramponi, G.; Dobson, C. M.; Stefani, M. *Nature* **2002**, *416*, 507.

(11) Arispe, N. *J. Membr. Biol.* **2004**, *197*, 33.

(12) Diaz, J. C.; Simakova, O.; Jacobson, K. A.; Arispe, N.; Pollard, H. B. *Proc. Natl. Acad. Sci. U.S.A.* **2009**, *106*, 3348.

(13) Kawahara, M.; Arispe, N.; Kuroda, Y.; Rojas, E. *Biophys. J.* **1997**, *73*, 67.

(14) Kayed, R.; Pensalfini, A.; Margol, L.; Sokolov, Y.; Sarsoza, F.; Head, E.; Hall, J.; Glabe, C. *J. Biol. Chem.* **2009**, *284*, 4230.

(15) Kayed, R.; Sokolov, Y.; Edmonds, B.; McIntire, T. M.; Milton, S. C.; Hall, J. E.; Glabe, C. G. *J. Biol. Chem.* **2004**, *279*, 46363.

(16) Lashuel, H. A.; Hartley, D. M.; Petre, B. M.; Wall, J. S.; Simon, M. N.; Walz, T.; Lansbury, P. T., Jr *J. Mol. Biol.* **2003**, *332*, 795.

(17) Mehta, P. D.; Pirttila, T.; Mehta, S. P.; Sersen, E. A.; Aisen, P. S.; Wisniewski, H. M. *Arch. Neurol.* **2000**, *57*, 100.

(18) Kuwahara, C.; Takeuchi, A. M.; Nishimura, T.; Haraguchi, K.; Kubosaki, A.; Matsumoto, Y.; Saeki, K.; Matsumoto, Y.; Yokoyama, T.; Itohara, S.; Onodera, T. *Nature* **1999**, *400*, 225.

(19) Narayan, P.; Orte, A.; Clarke, R. W.; Bolognesi, B.; Hook, S.; Ganzinger, K. A.; Meehan, S.; Wilson, M. R.; Dobson, C. M.; Klenerman, D. *Nat. Struct. Mol. Biol.* **2012**, *19*, 79.

(20) Johnson, R. D.; Schauerte, J. A.; Wisser, K. C.; Gafni, A.; Steel, D. G. *PLoS One* **2011**, *6*, e23970.

(21) Ding, H.; Wong, P. T.; Lee, E. L.; Gafni, A.; Steel, D. G. *Biophys. J.* **2009**, *97*, 912.

(22) Teplow, D. B.; Kheterpal, I.; Wetzel, R. *Methods Enzymol.* **2006**, *413*, 20.

(23) Edelstein, A.; Amodaj, N.; Hoover, K.; Vale, R.; Stuurman, N. *Curr. Protoc. Mol. Biol.* **2010**, *14*, 1.

(24) Tosatti, S.; Paul, S. M. D.; Askendal, A.; VandeVondele, S.; Hubbell, J.; Tengvall, P.; Textor, M. *Biomaterials* **2003**, *24*, 4949.

(25) VandeVondele, S.; Vörös, J.; Hubbell, J. A. *Biotechnol. Bioeng.* **2003**, *82*, 784.

(26) Csucs, G.; Michel, R.; Lussi, J. W.; Textor, M.; Danuser, G. *Biomaterials* **2003**, *24*, 1713.

(27) Shammas, S. L.; Waudby, C. A.; Wang, S.; Buell, A. K.; Knowles, T. P. J.; Ecroyd, H.; Welland, M. E.; Carver, J. A.; Dobson, C. M.; Meehan, S. *Biophys. J.* **2011**, *101*, 1681.

(28) Wilson, M. R.; Easterbrook-Smith, S. B. *Biochim. Biophys. Acta, Protein Struct. Mol. Enzymol.* **1992**, *1159*, 319.

(29) Crocker, J. C.; Grier, D. G. *J. Colloid Interface Sci.* **1996**, *179*, 298.

(30) Weimann, L.; Ganzinger, K. A.; McColl, J.; Irvine, K. L.; Davis, S. J.; Gay, N. J.; Bryant, C. E.; Klenerman, D. **2013**, submitted for publication.

(31) Qian, H.; Sheetz, M. P.; Elson, E. L. *Biophys. J.* **1991**, *60*, 910.

(32) Saxton, M. J.; Jacobson, K. *Annu. Rev. Biophys. Biomol. Struct.* **1997**, *26*, 373.

(33) Schütz, G. J.; Schindler, H.; Schmidt, T. *Biophys. J.* **1997**, *73*, 1073.

(34) Grünwald, D.; Martin, R. M.; Buschmann, V.; Bazett-Jones, D. P.; Leonhardt, H.; Kubitscheck, U.; Cardoso, M. C. *Biophys. J.* **2008**, *94*, 2847.

(35) Dunne, P. D.; Fernandes, R. A.; McColl, J.; Yoon, J. W.; James, J. R.; Davis, S. J.; Klenerman, D. *Biophys. J.* **2009**, *97*, L5.

(36) Bolognesi, B.; Kumita, J. R.; Barros, T. P.; Esbjorner, E. K.; Luheshi, L. M.; Crowther, D. C.; Wilson, M. R.; Dobson, C. M.; Favrin, G.; Yerbury, J. J. *ACS Chem. Biol.* **2010**, *5*, 735.

(37) Anderson, C. M.; Georgiou, G. N.; Morrison, I.; Stevenson, G.; Cherry, R. J. *J. Cell Sci.* **1992**, *101*, 415.

(38) James, J. R.; Vale, R. D. *Nature* **2012**, *5*, 7405.

(39) Mannini, B.; Cascella, R.; Zampagni, M.; van Waarde-Verhagen, M.; Meehan, S.; Roodveldt, C.; Campioni, S.; Boninsegna, M.; Penco, A.; Relini, A.; Kampinga, H. H.; Dobson, C. M.; Wilson, M. R.; Cecchi, C.; Chiti, F. *Proc. Natl. Acad. Sci. U.S.A.* **2012**, *109*, 12479.

(40) Yerbury, J. J.; Poon, S.; Meehan, S.; Thompson, B.; Kumita, J. R.; Dobson, C. M.; Wilson, M. R. *FASEB J.* **2007**, *21*, 2312.

(41) Narayan, P.; Meehan, S.; Carver, J. A.; Wilson, M. R.; Dobson, C. M.; Klenerman, D. *Biochemistry* **2012**, *51*, 9270.

(42) Charrier, C.; Ehrensperger, M. V.; Dahan, M.; Lévi, S.; Triller, A. *J. Neurosci.* **2006**, *26*, 8502.

(43) Andrews, N. L.; Lidke, K. A.; Pfeiffer, J. R.; Burns, A. R.; Wilson, B. S.; Oliver, J. M.; Lidke, D. S. *Nat. Cell Biol.* **2008**, *10*, 955.

(44) Abelein, A.; Bolognesi, B.; Dobson, C. M.; Gräslund, A.; Lendel, C. *Biochemistry* **2011**, *51*, 126.

(45) Campioni, S.; Mannini, B.; Zampagni, M.; Pensalfini, A.; Parrini, C.; Evangelisti, E.; Relini, A.; Stefani, M.; Dobson, C. M.; Cecchi, C.; Chiti, F. *Nat. Chem. Biol.* **2010**, *6*, 140.